



AMS

American Meteorological Society

Supplemental Material

[© Copyright 2018 American Meteorological Society](#)

Permission to use figures, tables, and brief excerpts from this work in scientific and educational works is hereby granted provided that the source is acknowledged. Any use of material in this work that is determined to be “fair use” under Section 107 of the U.S. Copyright Act or that satisfies the conditions specified in Section 108 of the U.S. Copyright Act (17 USC §108) does not require the AMS’s permission. Republication, systematic reproduction, posting in electronic form, such as on a website or in a searchable database, or other uses of this material, except as exempted by the above statement, requires written permission or a license from the AMS. All AMS journals and monograph publications are registered with the Copyright Clearance Center (<http://www.copyright.com>). Questions about permission to use materials for which AMS holds the copyright can also be directed to permissions@ametsoc.org. Additional details are provided in the AMS Copyright Policy statement, available on the AMS website (<http://www.ametsoc.org/CopyrightInformation>).

Irrigation Induced Land-Atmosphere Feedback and Their Impacts on Indian Summer Monsoon

Chihchung Chou¹, Dongryeol Ryu¹, Min-Hui Lo², Hao-Wei Wey², Hector Malano¹

¹Department of Infrastructure Engineering, University of Melbourne, Melbourne, Australia

²Department of Atmospheric Sciences, National Taiwan University, Taipei, Taiwan

Contents

Figure S1 to Figure S15 and Table 1

Text S1 IITM Rainfall Data Analyses

Text S2 Monthly climatology of irrigation water demand in 1991-2000

Text S3 Groundwater withdrawal

Text S4 Model stabilization and spin-up time

Text S5 Examination of monsoon index – rainfall anomaly

Text S6 Irrigation crop tiles

Introduction

This supporting information supplements some figures of simulation results from Figure S1 to Figure S15 Table 1 and some supporting details from Text S1 to Text S6.

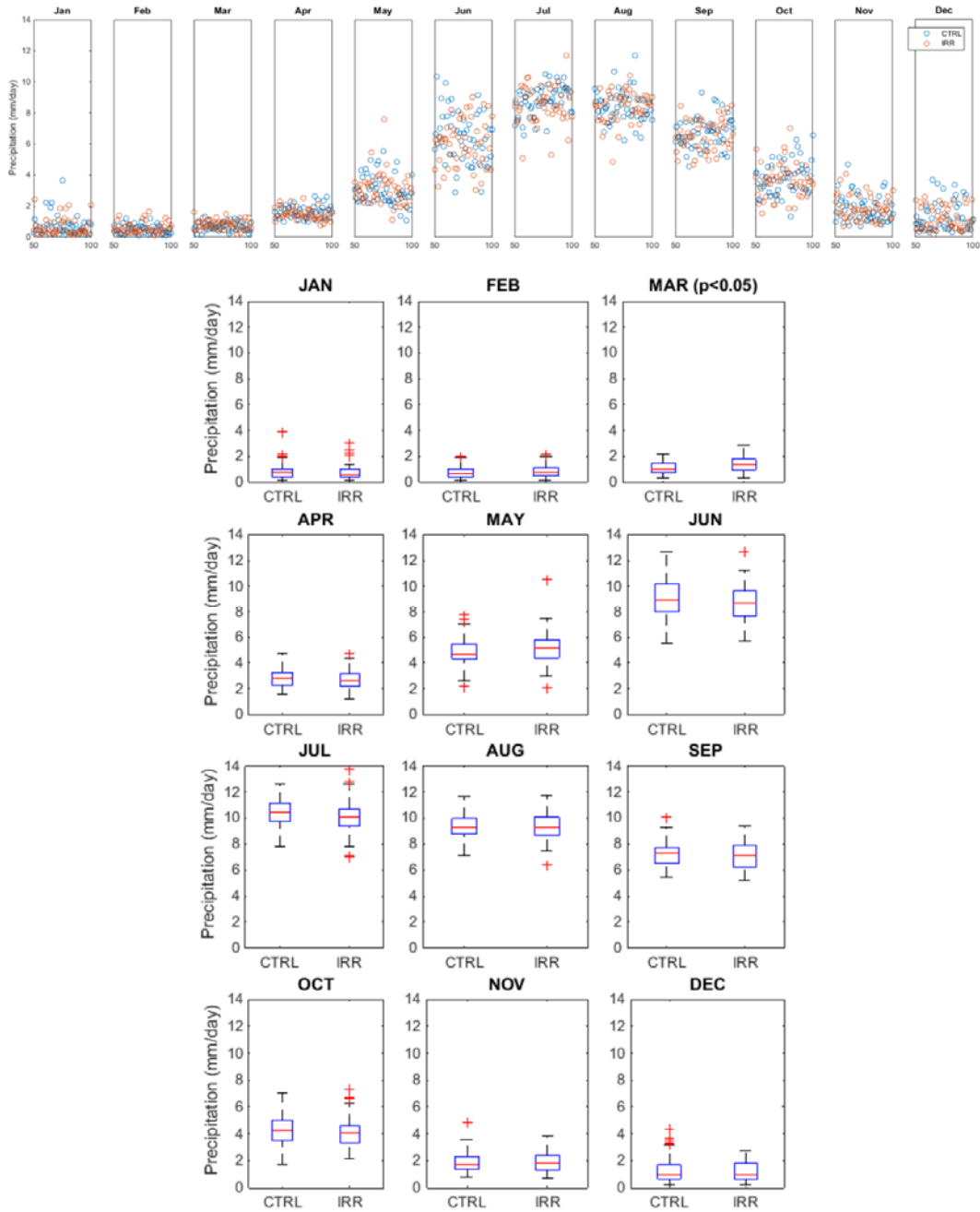


Figure S1. Fifty-year time series of monthly rainfall (upper) and comparison of the average monthly rainfall between CTRL and IRR cases (bottom).

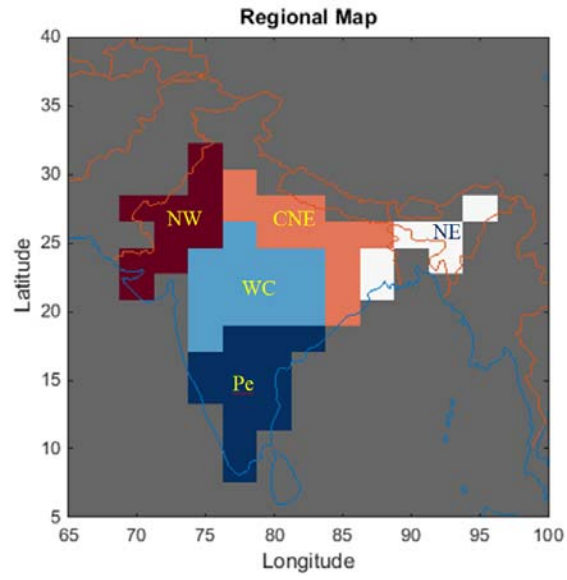


Figure S2. Map of subregions - NW (Northwest), NE (Northeast), CNE (Central-northeast), WC (West-central) and Pe (Peninsular) – used to sample sub-regional data in this work.

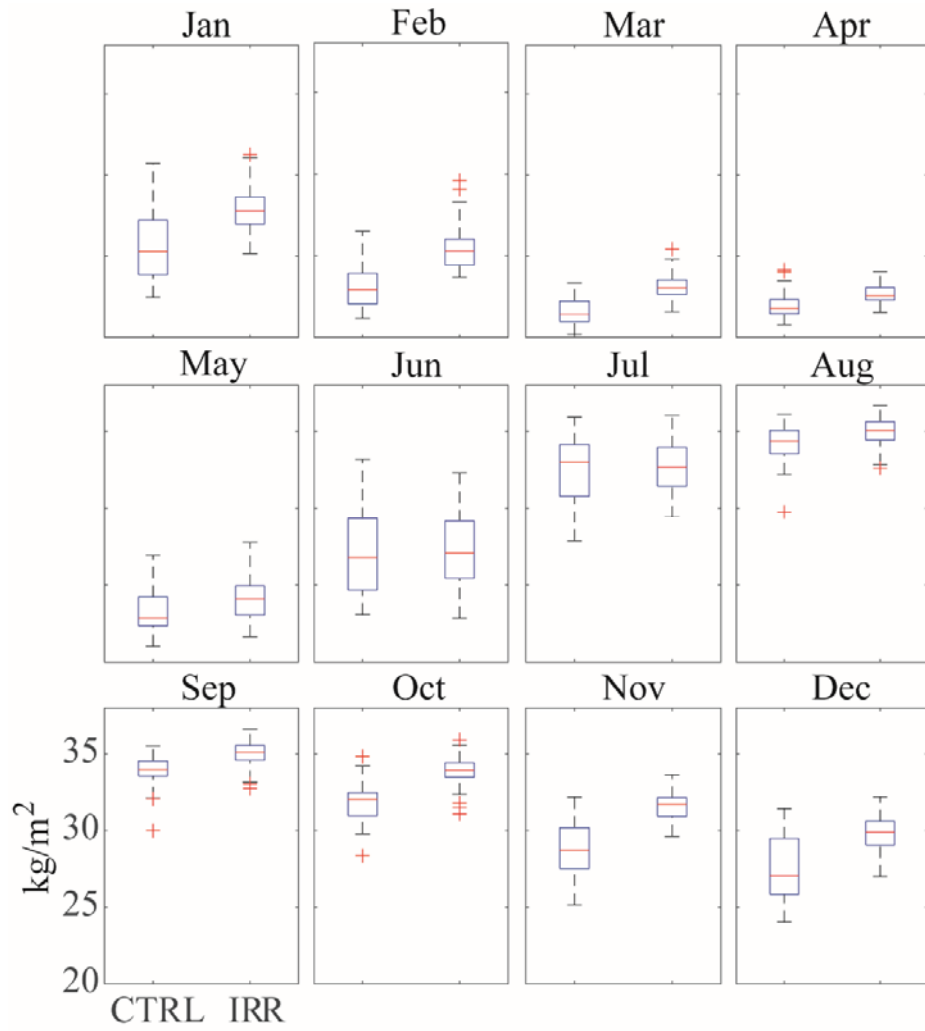


Figure S3. Comparison of monthly average SM between CTRL and IRR cases

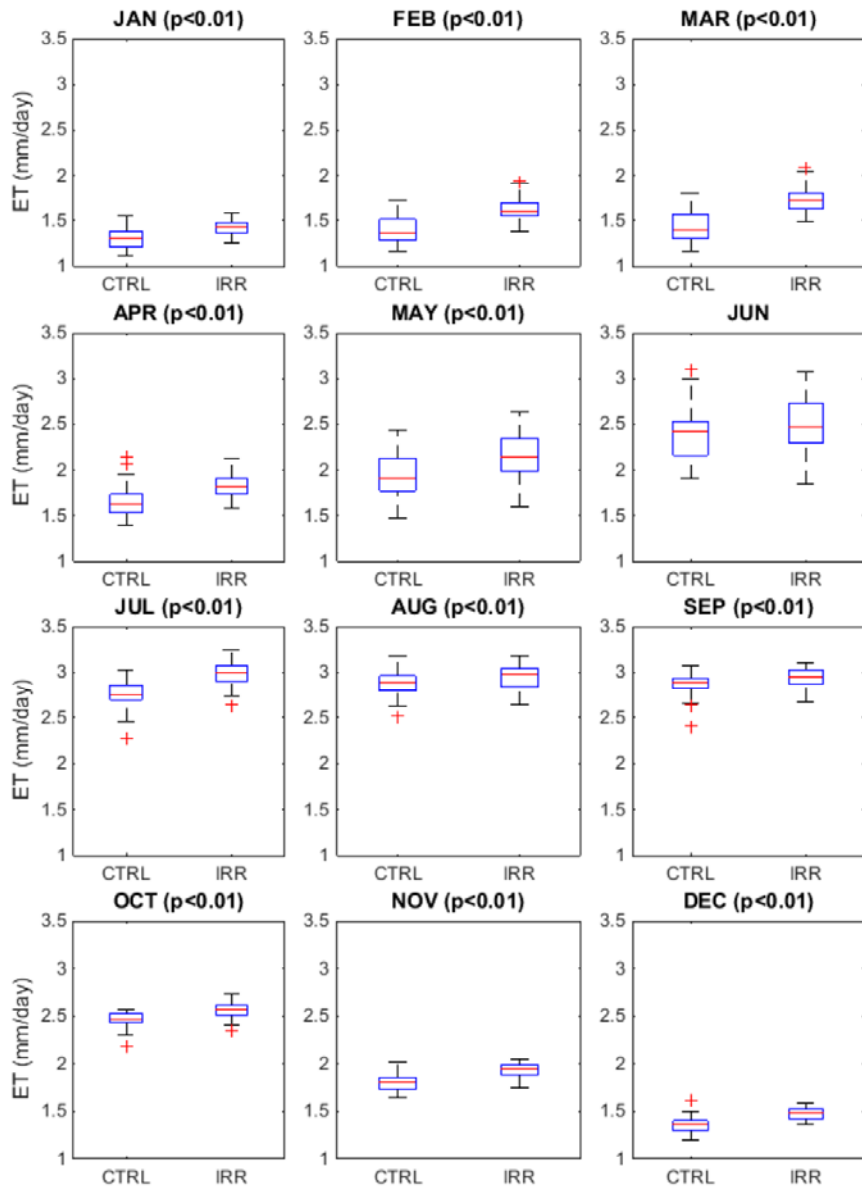
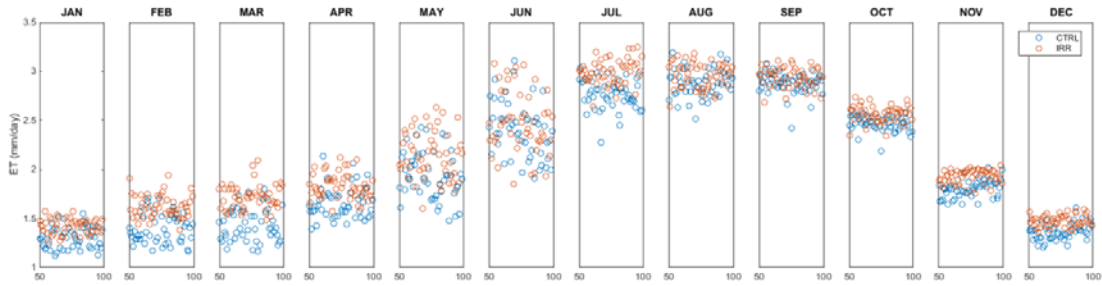


Figure S4. Fifty-year time series (upper) and comparison of monthly average ET (bottom) between CTRL and IRR cases

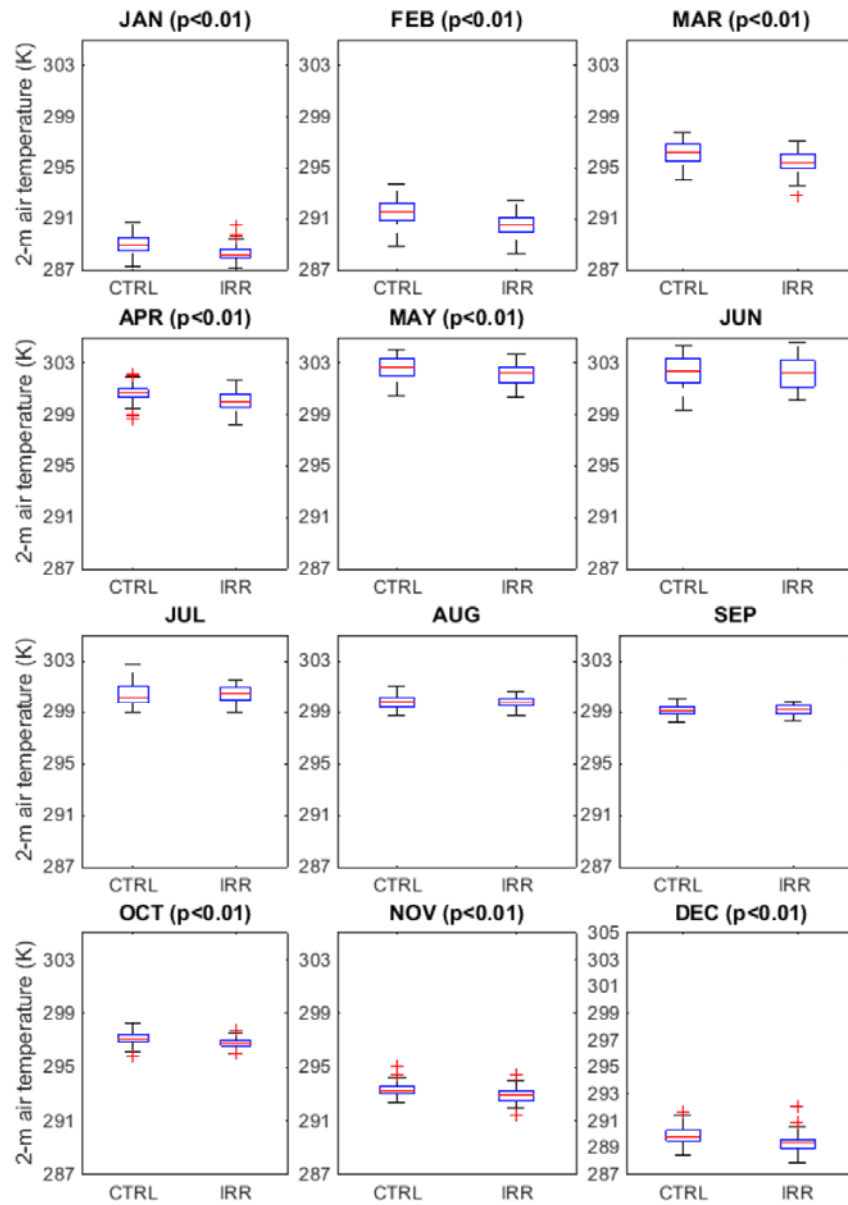
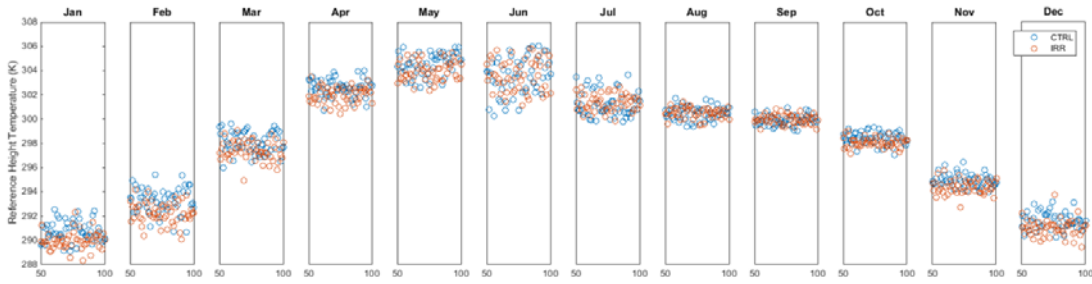


Figure S5. Fifty-year time series (upper) and comparison of monthly average 2-m temperature (bottom) between CTRL and IRR cases

Text S1 IITM Rainfall Data Analysis

Based on 306 rain gauge stations, IITM provides a long-term monthly rainfall record over all-India and other five sub-regions during 1871 and 2013 (see <http://www.tropmet.res.in/Home>). As shown in Figure S6, the JJAS rainfall and the 21-year moving-average time series are presented and the regions represented are clearly indicated using the central map. It is apparent that there are long-term cycles in 21-year moving average ISMR over all-India and each sub-region. To understand the long-term changes after substantial development of agricultural irrigation occurred from 1950s, the 21-year moving-average JJAS rainfall time series between 1881 and 1971 is considered as a training period for a cyclic rainfall model (sinusoidal function) with a linear long-term trend and the model is used to hindcast a long-term JJAS rainfall with no irrigation effect assumed in 1972-2003. Figure 5 and Table 1 illustrate that IITM data and model results are comparable in all regions except for the Northeast and Peninsular. Over northeast India, modelled rainfall does not show a statistically significant change in IRR case possible due to the high inter-annual variability as shown in Figure S7B. Over the Peninsular region, model tends to overestimate the JJAS rainfall comparing to observed records in Figure S7C and D. Overall, in most regions in India, the irrigation-related ISMR relative changes are consistent with the changes in IITM rainfall.

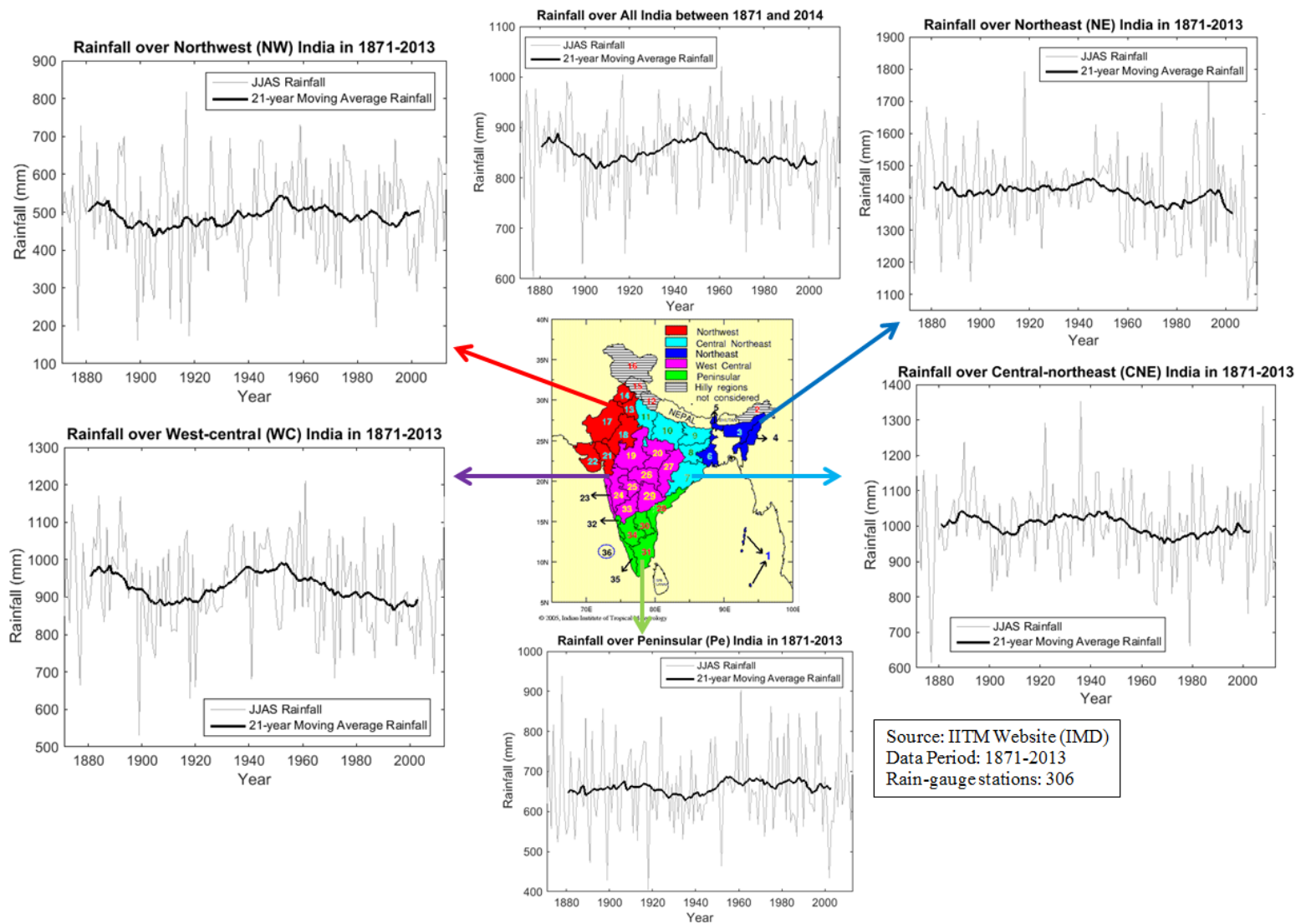


Figure S6. 21-year moving average JJAS rainfall over all-India and five sub-regions in 1871-2013

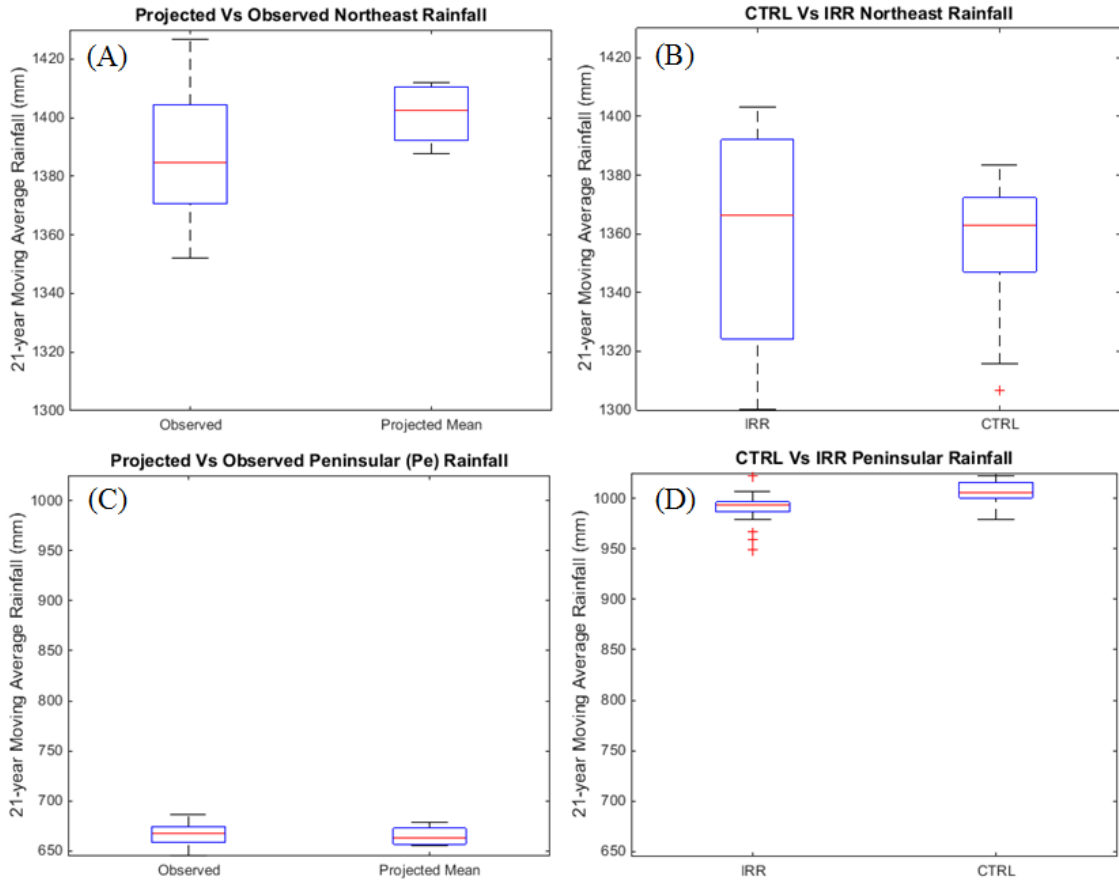


Figure S7. Comparisons of observed vs projected mean (left) and IRR vs CTRL (right) over the Northeast (upper) and Peninsular (bottom) region

Text S2 Monthly climatology of irrigation water demand in 1991-2000

The following characteristics reason the usage of the prescribed irrigation water demand data instead of being determined by the irrigation model in CLM:

- In CLM, the target soil moisture content (denoted SM hereafter) in CLM is a weighted value of the minimum SM (0.3) and the saturation SM (0.7). However, with precipitation data, the daily crop evapotranspiration with a time-varying crop physiological coefficient is estimated to determine the irrigation water demand (Wisser et al. 2008). The latter can better represent the theoretical irrigation water quantity instead of applying empirically chosen coefficient in each time step.
- When determining the area of irrigated cropland, the irrigation intensity is considered in *Wisser et al.* (2008), it, therefore, improves the estimation of irrigation water demand when the double cropping season exists.
- Using the meteorological conditions (i.e. temperature and precipitation) to determine the growing season would mimic a more realistic situation comparing with the criteria of crop leaf area (above zero or not) and photosynthesis (limited by water or not).

Figure S8 shows the comparison between the ‘climatological’ mean and CLM-derived annual irrigation water amount. The significantly different seasonal variability among the year indicates that August and September are the peak months of irrigation in the ‘climatological’ mean irrigation dataset while the CLM-derived irrigation dominates in April and May. Due to the lack of sub-annual irrigation water volume statistics, the seasonal variability of the simulated ET forced by the aforementioned two data sets is compared with the satellite product, AVHRR, and in-situ based dataset, Fluxnet. The intra-annual variability of ET would be substantially different if the irrigation water is applied within the totally different period of the year. Figure S9 shows the seasonal variability of ET from both simulation and observations,

only the ET forced by the CLM-derived irrigation water (the black dash line) peaks in June when the simulated ET forced by the ‘climatological’ mean irrigation (the blue and red dash lines) and two observational datasets (the purple and green lines) show highest values from July to September. Instead of the CLM-derived irrigation water, the gridded irrigation water demand dataset is applied in this study for the reasons mentioned above.

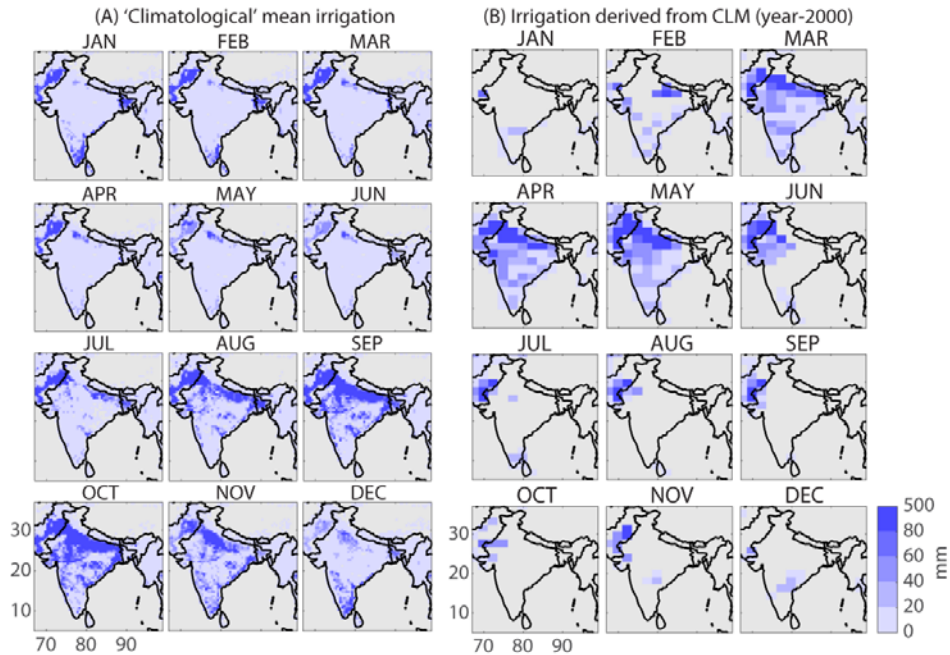


Figure S8. Comparison between the (A) ‘climatological’ mean and (B) CLM-derived annual irrigation water amount

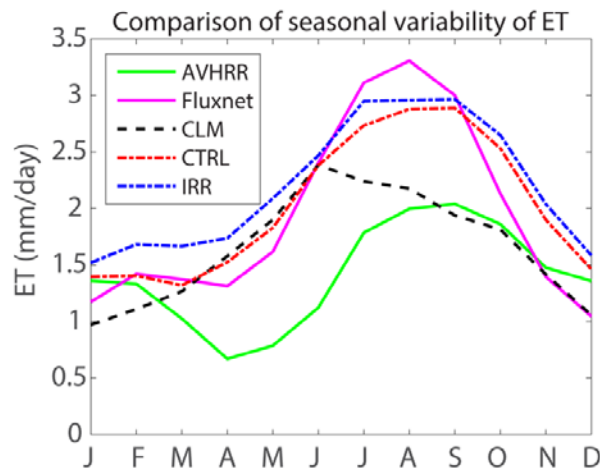


Figure S9. Comparison of seasonal variability of ET among five products

Using the monthly climatology would not be appropriate if there is a large inter-annual variability of irrigation over the study region. Therefore, we checked the inter-annual variability of annual irrigation in 1991-2000 as shown in the figures below. The standard deviation is 10% or less of the mean annual irrigation (grid-by-grid comparison, Figure S10B and C) over the entire India. In fact, *Wisser et al* (2008) indicated that their results are not historical, and should be viewed only as an estimate of inter-annual climate-driven variability in their setup of contemporary irrigation water use. Based on the small variation of the irrigation data in 1991-2000, we concluded that the mean values over 1991-2000 (used in this manuscript, Figure S10A) can be regarded as an acceptable estimate of the irrigation for our study. In the forecasting study, simulations with the low and high irrigation amounts should be undertaken to demonstrate the uncertainty of irrigation-induced effect on rainfall in the future study.

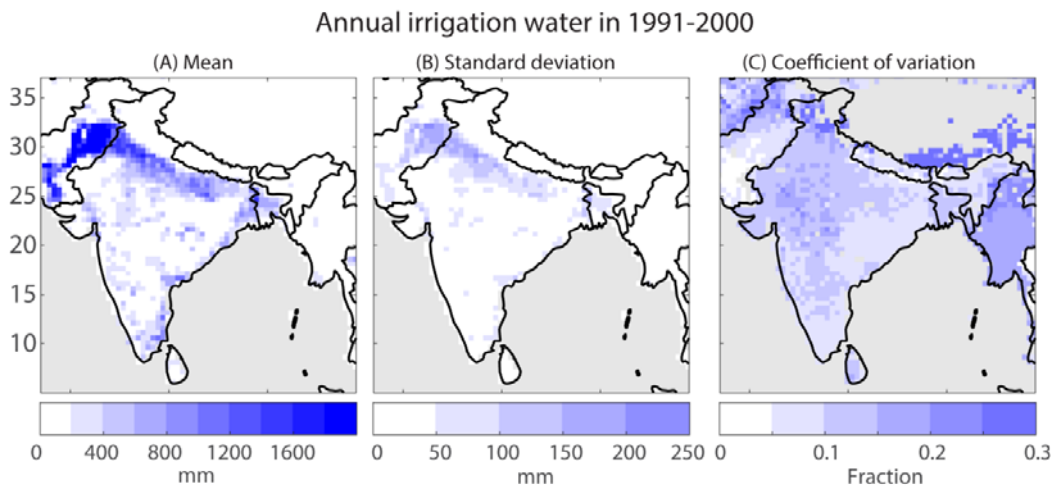


Figure S10. The spatial pattern of (A) mean, (B) standard deviation and (C) coefficient of variation of the annual irrigation water in 1991-2000

Text S3 Groundwater withdrawal

In terms of the irrigation water source in the simulation, we assumed that 50% of the irrigation water is from surface water, and the other half from groundwater in the simulation. However, the applied irrigation water is not subtracted from rivers, since the model does not simulate the evaporation of river water. As it is insignificant over the region of interest, water evaporation from lakes in the simulation is ignored. The monthly irrigation water amount is averagely distributed in each time step to mimic the flooding situation.

We followed Wey *et al.* (2015) and Siebert *et al.* (2010) who implied that around 50% of irrigation water is sourced from groundwater. The groundwater-sourced irrigation was extracted from the ‘unconfined aquifer’ of CLM (the land surface model within CESM), consequently the feedbacks to soil water and recharge rate should be propagated realistically as the reviewer comments. However, the higher variability of ratios of groundwater pumping for irrigation over different regions may raise uncertainties of changes in water balance affected by groundwater pumping.

Text S4 Model stabilization and spin-up time

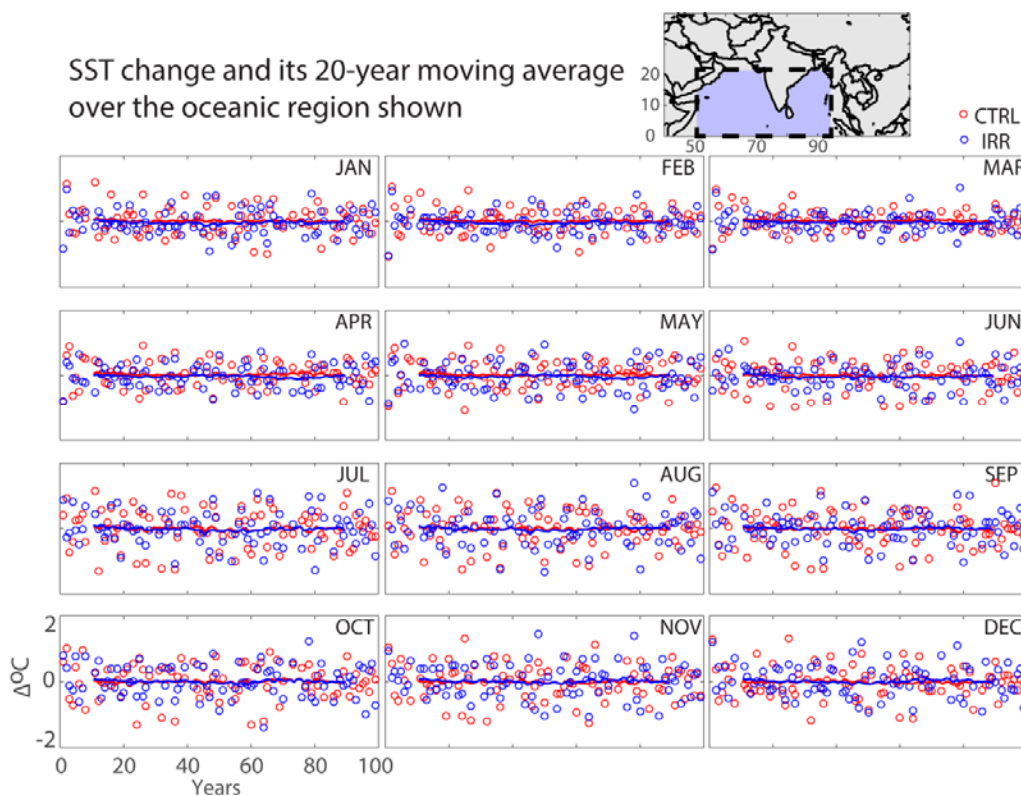


Figure S11. SST change and its 20-year moving average over the oceanic region (see inner plot)

Figure S12 shows the time series of 1-year-lag changes in SST by month over the oceanic region around the Indian subcontinent. For both of the cases, the 1-year-lag changes in SST fluctuate between $\pm 1^\circ\text{C}$ with trivial slope of $\leq 1.6 \times 10^{-3} \text{ }^\circ\text{C}/\text{year}$ and the 20-year moving average SST change ranges between with $\pm 0.2^\circ\text{C}$ standard deviation of $\leq 0.05^\circ\text{C}$. Therefore, considering the first 50-year as spin-up time is acceptable in this study when there is no trend observed. In addition, there is no significant difference of JJAS SST changes between two cases as shown in Figure S13. In addition, we also checked the Nino 3.4 SST as shown in Figure S15, and the result shows similar numbers of El-Nino years in both CTRL and IRR cases. Therefore, we think that considering the first 50 years as a spin-up period is acceptable, especially when

evaluating the irrigation-induced difference between two cases with the statistical significance test.

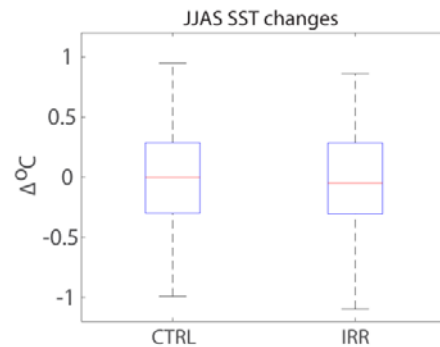


Figure S13. JJAS SST changes summarised from Figure S14 **Error! Reference source not found.**

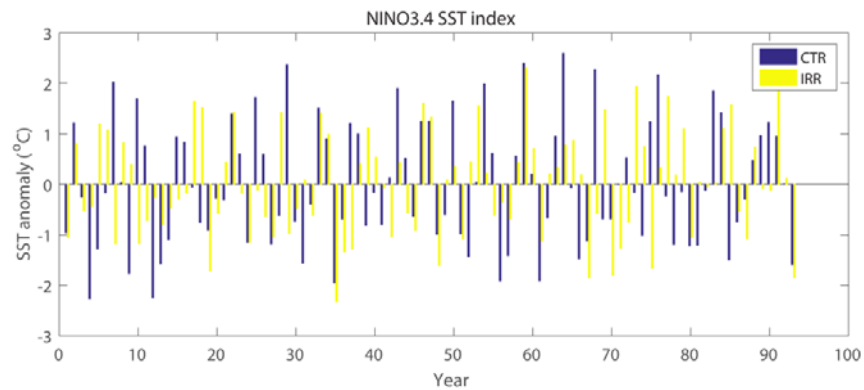


Figure S15. Nino 3.4 SST index - anomaly

CESM typically produces variable outputs even with the same annual forcing input (i.e., CO₂, aerosols, land cover and land use change, etc. at the year-2000 level in this study). Although the rainfall in Figure 4B appears to be fluctuating with a trend in CTRL case, the actual variability is within an acceptable range (20-40 mm). Furthermore, we checked the entire period of simulation and the variability shows a modelled fluctuation with an insignificant trend (slope ~ 0.0021). Therefore, the visual impression largely originates from the vertical scale of the original figure. On the other hand, the IRR case presents rainfall with a more pronounced trend (slope ~ 0.0105) which indicates a transient state in progress with the treatment (i.e.,

irrigation), but it also varies within a similar range like CTRL case. On top of the modelled fluctuation found in both cases, the IRR case still well presents the effect of irrigation on rainfall. Therefore, the relative reduction of rainfall from CTRL to IRR case is regarded as the changes resulted from irrigation.

Text S5 Examination of monsoon index – rainfall anomaly

There are several monsoon indexes used in previous works, including the Rainy Day and Daily Intensity (Revadekar and Preethi 2012), the Seasonality Index (Guhathakurta and Saji 2013) and the Rainfall Anomaly (Gadgil and Joseph 2003). The first two indexes would be more suitable for daily data, and the third index is to examine the rainfall regime. Next, the rainfall anomaly is related to monsoon strength and more suitable for the monthly or annual rainfall dataset. Therefore, we use the rainfall anomaly to check the irrigation-induced changes over the northwest India where the rainfall shows the most significant reduction in Figure 2.

In Table 1, the irrigation-induced rainfall anomaly has decreased in June, July and September from the CTRL case to the IRR case while there is a slightly increase in August. The decreases in the rainfall anomaly in June and July is consistent with our conclusion that it is associated with the weakened summer monsoon wind caused by the reduced land-sea thermal contrast. On the other hand, the combined effect of the two competing feedbacks possibly reduce the negative influence on rainfall resulted from irrigation in August and September. Here, the rainfall anomalies show slight increase/decrease in Table 1.

Table 1 Average Rainfall anomaly in JJAS over the Northwest India in both cases

	JUN	JUL	AUG	SEP
CTRL	2.27×10^{-18}	1.05×10^{-16}	-1.59×10^{-17}	-1.37×10^{-16}
IRR	-2.62×10^{-16}	-1.76×10^{-16}	-1.44×10^{-17}	-1.74×10^{-16}

Text S6 Irrigation crop tiles

The irrigation water quantity was applied to the entire grid. The large spatial support (grid size) of the current simulation can be problematic when it is used to reproduce surface processes nonlinearly related to soil moisture. However, the mean latent heat release over the Indo-Gangetic Plain region is 37.74 W/m^2 in the IRR case which is comparable to two ET products (the satellite-derived AVHRR-based ET and the in situ-based FLUXNET-Based ET averaged in 1983-2006 and 1982-2011, respectively) during wintertime (Wey et al. 2015). Also, we compared the ET among three products (FLUXNET-based, CTRL and IRR) as shown below, ET increases from the CTRL to IRR case during summertime and is comparable with the in situ-based product. Furthermore, over the region of interest, the net irrigated areas account for 44% of the States' area over northwest India (including States of Punjab, Haryana, Gujarat and Rajasthan), especially 80% in Punjab. The effect of irrigation on non-irrigation crop tiles, therefore, is supposed to be negligible in this case.

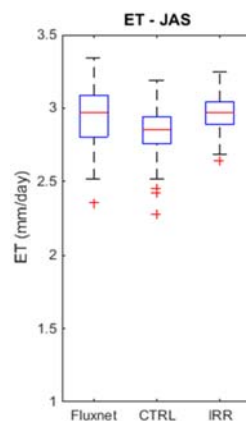


Figure S16 Comparison of JAS ET between FLUXNET, CTRL and IRR products

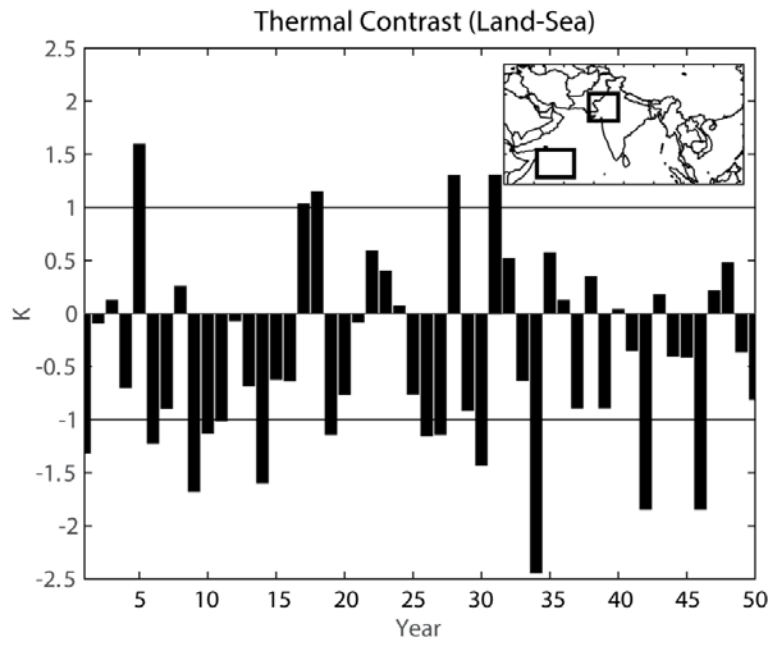


Figure S15 Irrigation-induced (IRR-CTRL) change in land-sea thermal contrast

References

Gadgil, S., and P. Joseph, 2003: On breaks of the Indian monsoon. *Journal of Earth System Science*, **112**, 529-558.

Guhathakurta, P., and E. Saji, 2013: Detecting changes in rainfall pattern and seasonality index vis-à-vis increasing water scarcity in Maharashtra. *Journal of Earth System Science*, **122**, 639-649, doi:10.1007/s12040-013-0294-y.

Revadekar, J., and B. Preethi, 2012: Statistical analysis of the relationship between summer monsoon precipitation extremes and foodgrain yield over India. *International Journal of Climatology*, **32**, 419-429, doi:10.1002/joc.2282.

Siebert, S., J. Burke, J.-M. Faures, K. Frenken, J. Hoogeveen, P. Döll, and F. T. Portmann, 2010: Groundwater use for irrigation—a global inventory. *Hydrology and Earth System Sciences*, **14**, 1863-1880, doi:10.5194/hess-14-1863-2010.

Wey, H. W., M. H. Lo, S. Y. Lee, J. Y. Yu, and H. H. Hsu, 2015: Potential impacts of wintertime soil moisture anomalies from agricultural irrigation at low latitudes on regional and global climates. *Geophysical Research Letters*, **42**, 8605-8614, doi:10.1002/2015GL065883.

Wisser, D., S. Frohking, E. M. Douglas, B. M. Fekete, C. J. Vörösmarty, and A. H. Schumann, 2008: Global irrigation water demand: Variability and uncertainties arising from agricultural and climate data sets. *Geophysical Research Letters*, **35**, doi:10.1029/2008GL035296.